Proceedings of the 28th IEEE
EMBS Annual International Conference
New York City, USA, Aug 30-Sept 3, 2006

Quantitative small animal fluorescence tomography using an ultra-fast gated image intensifier

Sachin V. Patwardhan, Sharon Bloch, Samuel Achilefu, and Joseph P. Culver

Abstract— **Optical approaches to small animal in vivo molecular imaging provide high sensitivity, stable non-radioactive probes, and an extensive array of functional reporting strategies. However, quantitative whole body assays remain illusive. The quantitative accuracy of optical imaging is affected by the depth of the buried target and the heterogeneity of tissue optical properties. Tomography approaches, to obtaining in-vivo optical property maps, and whole body distributions of fluorescing probes, provide a strategy for improving the quality and quantitative accuracy of small animal optical imaging. Here we present a time-resolved, charged coupled device (CCD) based system for quantitative small animal fluorescence tomography.**

III. Introduction

IMAGING biochemical events with near infrared fluorescent agents provides an attractive new approach for studying models of human diseases in live small animals. The potential benefits of whole-body optical tomography are significant and particularly relevant to cancer models involving internal organs. With recent advances in targeted fluorescence optical probes, and diffuse optical tomography (DOT) methods, quantitative three dimensional assays of probe activity *in vivo* are now feasible. Tomographic approaches to small animal *in vivo* fluorescence and bioluminescence imaging address some of the limitations of planar reflectance techniques by providing quantitative strategies that can account for partial volume effects, reduce the influence of superficial tissue, and improve the contrast-to-noise ratio (CNR) of buried targets.

Feasibility of *in vivo* continuous-wave fluorescence tomography (CWFT) has been demonstrated in small animals [1-2]. The prototype fast scanning CWFT system [2] that we recently reported uses galvanometric mirror pairs to raster scan the source with flexible and dense spatial sampling. Large field-of-view and short scan times allows us to measure probe kinetics, retention, clearance pathways, and localization of targeted agents throughout the small animal body. This system provides a sensitivity of 1 nM concentration (100 femtomoles) and a linear measure from 1 nM to 1 μM concentrations of the fluorescent agent.

Generally, *in vivo* CWFT involves differential measurements of emitted fluorescence light intensity over the re-emitted excitation light intensity. Differential measurements significantly reduce the influence of heterogeneous optical properties and path lengths and thus far, small animal fluorescence tomography studies have generally assumed homogeneous optical properties. However the optical properties of small animals are strongly heterogeneous. Fig. 1 shows the transmitted light intensities measured by opposite source-detector pairs along the longitudinal axis of a mouse body as indicated by the dashed line on the white light mouse image. A variation of about 2 orders in magnitude can be observed in the transmitted light intensity. Light intensity is low near the heart region due to large absorption by hemoglobin while it is high in the abdominal region. This indicates that the optical properties in the mouse vary by an order of magnitude or more. Such heterogeneity in the optical properties can significantly degrade the image quality of fluorescence tomography images if homogenous optical properties are assumed[cite osa abstract].

Methods of obtaining the subject specific optical properties are desired and can in principal be obtained using temporally resolved measurements, either with frequency-domain [4] or time-domain modulation [5-6]. To take advantage of CCD spatial sampling and achieve good temporal resolution, image intensifiers (ICCD) have been used with both frequency-domain [7] and time-domain [8-9] approaches. The use of ICCD tomography systems, however, has been focused primarily on imaging fluorescence lifetimes [7], using early time gates for increased spatial resolution [9] or late gates for increased depth penetration [8]. Further, the frequency domain measurements for independent tomographic maps of absorption and scattering have generally been limited to large tissue volumes [4,7] and modulation frequencies of <300 MHz. For small animal measurements with short source-detector separations, the measured pulse delays are expected to be small, suggesting that the use of higher modulation frequencies might be beneficial.

Manuscript received April 3, 2006. This work was supported in part by the National Institutes of Health grants, K25-NS44339, BRG R01and CA109754, and Small Animal Imaging Resource Program (SAIRP) grant, R24 CA83060.

S. V. Patwardhan is with the Washington University School of Medicine, Department of Radiology, Saint Louis, MO 63110 USA (phone: 314-362-6942; fax: 314-747-5191; e-mail: patwardhans@mir.wustl.edu).

S. Bloch is with the Washington University School of Medicine, Department of Radiology, Saint Louis, MO 63110 USA (e-mail: blochs.@wustl.edu.).

S. Achilefu is with the Washington University School of Medicine, Department of Radiology, Saint Louis, MO 63110 USA (e-mail: achilefus@wustl.edu).

J. P. Culver is with the Washington University School of Medicine, Department of Radiology, Saint Louis, MO 63110 USA (e-mail: culverj.@wustl.edu.).

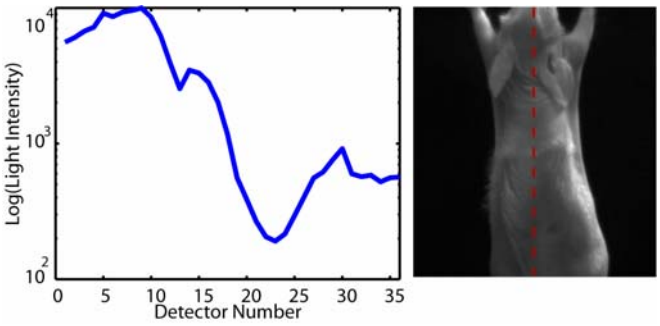

Fig. 1. Transmitted light intensities measured by opposite source-detector pairs along the longitudinal axis of a mouse body as indicated by the dashed line on the white-light mouse image.

We present here a time-resolved, ICCD-based tomography system for obtaining quantitative absorption and scattering optical property maps in small animals. Using Fourier-transformed time-domain data, we show that measurements with useful contrast-to-noise ratios can be obtained with modulation frequencies up to 1 GHz. Experiments in tissue simulating phantoms are used to demonstrate the feasibility of reconstructing volumetric optical properties with the derived frequency domain data.

IV. Methods

The CWFT system presented in [2] was modified for time resolved measurements by incorporating a pulsed laser source and an image intensifier as illustrated in Fig. 2. For testing the feasibility of reconstructing absorption and scattering maps, a tissue-like phantom was formed using two 3.5mm (OD) tubes filled with Intralipid™, water, and, India ink mixture to mimic an absorbing (μ_a=0.4cm^{-1}, μ_s'=10cm^{-1}) object and a scattering (μ_a=0.1cm^{-1}, μ_s'=40cm^{-1}) object. The tubes were suspended in the imaging cassette filled with matching fluid (μ_a=0.1cm^{-1}, μ_s'=10cm^{-1}) and were separated by a center-to-center distance of 2cm. Phantom and background data were collected by scanning the imaging cassette with and without the phantom using 24 symmetrically arranged source detector pairs with 2mm spacing. For each source position 32 time resolved measurements were obtained by sampling the laser pulse at 100ps with the image intensifier gate width of 400ps.

The measurement setup is illustrated in Fig. 3a. This figure also illustrates the concept of time-resolved measurements where the pulsed laser illuminates the imaging cassette and the gated intensifier time-resolves samples of the light emitted from the opposing window. Due to scattering and absorption, the detected pulse has decreased intensity and is delayed; its dependence on source-detector separation is illustrated. The system response function (Fig. 3b) with time t=0s is shown along with the response to a homogeneous medium as measured by 3 equally spaced detectors with increasing source-detector separation. The signal amplitude falls off exponentially with increasing source-detector separation, while the mean time-of-flight increases with distance, reflecting an increase in mean path length with increased source-detector distance.

For reconstruction, the data was converted from time-domain to frequency domain using Fourier transform technique for modulation frequencies of 312.5, 625, and 1250 MHz. The signal amplitude and phase for the three modulation frequencies (312.5 MHz (blue), 625 MHz (green), and, 1250MHz (red)) obtained from background measurements are shown in Fig. 3c and Fig. 3d, respectively, for the 12th source and all detectors (2 mm spacing). Frequency domain data was similarly obtained for the measurements with and without the phantom targets. We perform a linear reconstruction solution by inverting the perturbation equation y=Ax. Here, y is the differential measurement vector obtained by taking the negative log of the ratio of light intensities with and without the phantom targets on the detector plane. The optical property map, x =[x_a; x_s] is represented as a vector of voxels with x_a and x_s as the absorption and the scattering components, and the sensitivity matrix is A = [A_a A_s], where A_a and A_s are the first order derivatives of the fluence with respect to absorption and scattering. The inverse problem is solved using a Moore-Penrose generalized inverse.

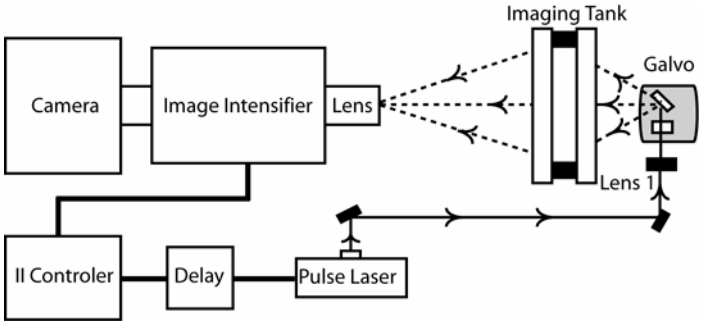

Fig. 2. Schematic of the temporally resolved fluorescence tomography system. A pulsed laser source (Becker&Hickel, BHLP-700) delivers 780nm, 50 MHz, T_p=100ns, 3mW laser pulses. The beam, after passing through the focusing lens (Lens1), is steered by pair of galvanometer scanning mirrors (Galvo) to the source side of the imaging tank. Light emitted from the detector plane of the imaging cassette is filtered and collected by a lens and temporally gated by an ultra-fast gated imaged intensifier (PicoStarHR-12, LaVision,(τ_{gate}<300ps)). This temporally gated image is then relayed to an EMCCD camera (iXon 877f, Andor Technologies) for read out. Timing between the source and the gated detection is controlled by the trigger pulse received from the pulsed laser source, which is passed through a programmable delay unit to the ultra-fast high voltage image intensifier control.

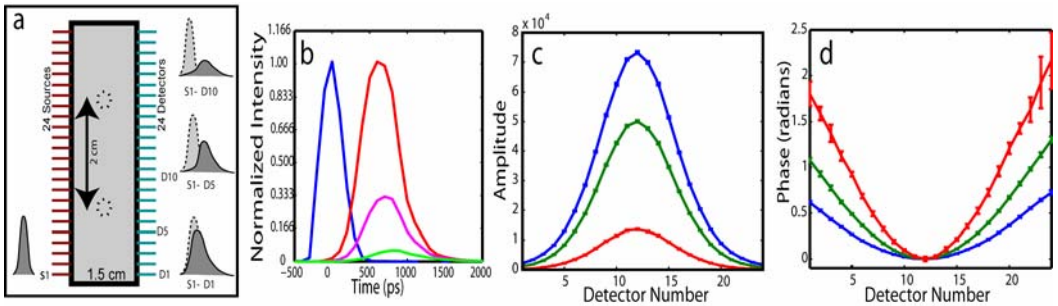

Fig. 3. Measurement setup and conversion of time-resolved measurements to frequency domain data using Fourier transform. (a) The concept of time-domain measurement is illustrated–the input laser pulse is delayed and broadened when sampled on the detector window. Two phantom targets are placed at the center of the imaging cassette and scanned using 24 source and 24 detector positions. (b) The system response function with time t=0s is shown along with the response to a homogeneous medium as measured by 3 equally spaced detectors with increasing source-detector separation. The signal amplitude (c) and phase (d) for three modulation frequencies, 312.5 MHz (blue), 625 MHz (green), and, 1250 MHz (red), are calculated by Fourier transform of the time domain measurements (data shown for the 12th source and all the detectors).

III. Results and Discussion

Temporally resolved data was collected for each of 24 source positions and at 24 detector positions. The measurements were then Fourier transformed into frequency domain data. Using a shot noise model with the noise proportional to the square root of the intensity, we weighted the data by the SNR of the light intensity measurements. In Fig. 4 a- b, the noise weighted differential amplitude and phase for a modulation frequency of 625 MHz are depicted as images in which each pixel represents a source-detector pair. It can be seen from the figures that a good contrast can be obtained for both the absorbing and scattering tubes. The amplitude of the scatter wave is negative for both the scattering and absorbing objects while the phase shows an increased delay for the scattering object (upper left) and decreased delay for the absorbing object (lower right). Reconstructions of the absorption (Fig. 4c) and scattering (Fig. 4d) perturbations demonstrate the capability to separate the two optical properties. Since one tube has the same absorption as the surrounding but 4x more scattering, while the other tube has the same scattering as the surrounding but 4x more absorption, only one tube shows up in either of the reconstructed components. Similar reconstructions where obtained from 312.5 and 1250.MHz modulation frequency data sets.

IV. Conclusions

The data presented demonstrate the feasibility of reconstructing the optical property maps of small tissue volumes from high frequency time-resolved amplitude and phase data. Useful contrast-to-noise ratios were obtained even for modulation frequencies in the range of 300-1250 MHz and absorption and scattering components were successfully reconstructed and separated using 625 MHz data. The *in situ* heterogeneous optical property maps obtained with this diffuse optical tomography system can be used as a basis for quantitative fluorescence tomography of small animals. Use of an ICCD permits integration of this approach into our existing CW small animal fluorescence tomography system. Compared to fluorescence reconstructions using homogeneous tissue models, tomographic images obtained using heterogeneous tissue models are expected to provide a more uniform sensitivity function throughout the reconstructed volume. We are presently evaluating the selection of modulation frequencies for optimal reconstruction of small animal optical properties.

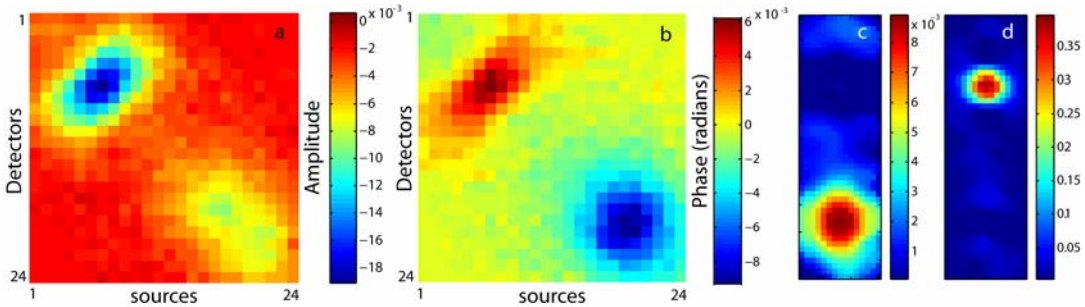

Fig. 4. Frequency domain data and reconstructions using 625 MHz modulation frequency. (a and b) Amplitude and phase of the noise weighted differential measurements as an image for the 24x24 source-detector grid where each pixel represents a source-detector pair. The diagonal represents opposing source-detector pair measurements. The absorbing object (lower right corner) has decreased amplitude and a negative phase delay while the scattering object (upper left corner) has decreased amplitude with a positive phase delay. (c-d) 2D representative slices of the absorption and scattering components respectively. These slices are obtained from 3D reconstruction of the frequency domain phantom data set at 625 MHz modulation frequency.

REFERENCES

[1] Ntziachristos, V. and R. Weissleder, "Charge-coupled-device based scanner for tomography of fluorescent near-infrared probes in turbid media," Med. Phys. 29, 803-809 (2000).

[2] Patwardhan, S.V., S.R. Bloch, S. Achilefu and J.P. Culver, "Time-dependent whole-body fluorescence tomography of probe bio-distributions in mice," Optics Express, 2005. 13(7): p. 2564- 2577.

[3] Arridge, S.R. and W.R.B. Lionheart, "Nonuniqueness in diffusion-based optical tomography," Optics Letters, 1998. 23(11): p. 882-884.

[4] McBride, T.O., B.W. Pogue, S. Jiang, U.L. Osterberg and K.D. Paulsen, "A parallel-detection frequency-domain near-infrared tomography system for hemoglobin imaging of the breast in vivo," Review of Scientific Instruments, 2001. 72(3): p. 1817-1824.

[5] Schmidt, F.E.W., M.E. Fry, E.M.C. Hillman, J.C. Hebden and D.T. Delpy, "A 32-channel time-resolved instrument for medical optical tomography," Review of Scientific Instruments, 2000. 71(1): p. 256-265.

[6] Ntziachristos, V., X.H. Ma, A.G. Yodh and B. Chance, "Multichannel photon counting instrument for spatially resolved near infrared spectroscopy" Review of Scientific Instruments, 1999. 70(1): p. 193-201.

[7] Thompson, A.B. and E.M. Sevick-Muraca, "Near-infrared fluorescence contrast-enhanced imaging with intensified charge-coupled device homodyne detection: measurement precision and accuracy," Journal of Biomedical Optics, 2003. 8(1): p. 111-120.

[8] Selb, J., J.J. Stott, M.A. Franceschini, A.G. Sorensen and B. DA, "Improved sensitivity to cerebral hemodynamics during brain activation with a time-gated optical system: analytical model and experimental validation," Journal of Biomedical Optics, 2005. 10(1): p. 0110131-01101310.

[9] Turner, G.M., G. Zacharakis, A. Soubret, J. Ripoll and V. Ntziachristos, "Complete-angle projection diffuse optical tomography by use of early photons," Optics Letters, 2005. 30(4): p. 409-411.